PCCP

Accepted Manuscript

ROYAL SOCIETY OF CHEMISTRY

www.rsc.org/pccp

Effect of junction mode between backbone and side chain of polyimide on stability of liquid crystal vertical alignment

Xinyuan Che[a], Shiming Gong[a], Heng Zhang[a], Bin Liu[a] and Yinghan Wang[*a]

Abstract:

Polyimides (PI-N9 and PI-N12) were synthesized from two kinds of functional diamines, whose junction modes between backbones and side chains were different. Side chains of PI-N9 were linked to the backbones with an ether bond spacer; and side chains of PI-N12 were directly linked to the backbones without any spacer. The PI alignment layers surfaces were investigated by atomic force microscopy, surface free energy measurement, X-ray photo-electron spectroscope and polarized attenuated total reflection flourier transformed infrared spectroscopy. It was found that the PI-N9 lost the vertical alignment capability after high-strength rubbing, while the PI-N12 could still induce liquid crystals (LCs) to align vertically under the same condition. The mechanism of the macroscopic molecular orientation of the PIs surface is proposed. During the high-strength rubbing process, the side chain could rotate around the flexible ether bond which existed between the side chain and the main chain of PI-N9 and then fell over. Therefore, the PI-N9 could not induce the vertical alignment of LCs anymore. But PI-N12 could keep LCs aligning vertically all the time, which proved that the stability of LC alignment induced by PI-N12 was better.

[a] *State Key Laboratory of Polymer Materials Engineering of China, College of Polymer Science and Engineering, Sichuan University, Chengdu 610065, China.*

*Corresponding author. E-mail: wang_yh@scu.edu.cn

1. Introduction

Polyimides (PIs) have been widely used in many technical applications due to their advantageous properties, such as heat resistance, dimensional stability, mechanical and dielectric properties, and so forth.[1-3] One of the most important applications is using as liquid crystal (LC) alignment layers in the manufacture of flat-panel LC display (LCD) devices. Prior to use, the PIs film surfaces need to be treated to unidirectionally align the LC molecule.[4-5] Among the alignment technology of LCs, rubbing has been the most widely used method due to its simplicity, low cost, and the controllability.[6-9] After the rubbing process, a defined range of pretilt angle can be obtained. The pretilt angle plays the most predominant role in determining the optical and electrical performance of the industrial LCD devices.[10-12] Compared with the conventional twisted nematic LCDs which needed only a low pretilt angle, vertical alignment LCDs which requested a pretilt angle above 89° after a rubbing process has wide viewing angle, high contrast ratio and fast response time.[13,14] For the vertical alignment technology, not only the specific chemical structure but also the rubbing process has great influence on uniform alignment of LCs.[15-17] What's more, the stability of LC vertical alignment is particularly important to the vertical alignment LCDs. If the high pretilt angle could not be maintained after rubbing, the LCD would lose its high performance.

It was reported that long alkyl side chains contributed to achieving a high pretilt angle.[18] Many previous researchers studied effect of molecular structure of PIs containing side chains on the pretilt angle and conformation. Sakai *et al*. pointed out that a high pretilt angle was achieved using PIs with bulky side chains composed of rigid units and long alkyl chains as the alignment layer.[19] Lee *et al*. further confirmed that the PI with rigid alicyclic and flexible alkyl group side chain could align the LC vertically after the rubbing process.[20] Guo *et al*. manifested length and contents of the side chain are crucial factors in the conformation of the side chains and the vertical alignment of LCs.[21] Wang *et al*. concluded that the chemical groups in the surface taking a vertical conformation on the surface play an essential role in producing a vertical LC alignment and the conformation of groups in the surface determines the size of pretilt angle.[22] However, the effect of junction mode between backbone and side chain of PI on stability of LC vertical alignment has never been researched. Besides, mechanism of LC vertical alignment on PIs film has not been carefully

investigated.

In this study, two kinds of PIs (PI-N9 and PI-N12) whose side chains were linked to the backbones in different ways (for PI-N9, linked with an ether bond spacer; for PI-N12, directly linked without any spacer) were synthesized from different functional diamines. They had the same backbone and similar side chains composed of rigid and flexible units. As shown in the Fig. 1, the length of N, N-bis (4-aminophenyl)-4-(nonyloxy-biphenyl)-4'-aminophenyl ether (N9) and 4-dodecyloxy-biphenyl-4',4"-diaminotriphenylamine (N12) were 24.368 and 24.504 Å, respectively (The structure geometries of two functional diamines were optimized by the density functional theory [B3LYP/6-311G (d,p)] calculations using a large basis-set function).[23] The effect of changing the rubbing strength on the alignment of the liquid crystal was researched, we found an interesting phenomenon: before rubbing, all the PI alignment layers could induce LCs to align vertically; after a certain number of rubbing, some of them lost the vertical alignment capability, but some of them were not. Deep understanding of the effect of the way in which side chains are linked to backbones on stability of LC vertical alignment will contribute to controlling the pretilt angle better. Therefore, the PI film surfaces were investigated by atomic force microscopy (AFM), surface free energy measurement, X-ray photo-electron spectroscope (XPS) and polarized attenuated total reflection flourier transformed infrared spectroscopy (ATR-FTIR).

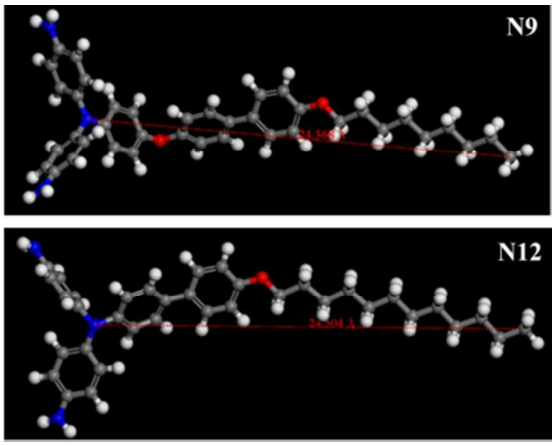

Fig. 1 The optimal geometric conformation diagram of two functional diamines. Gray, white, red and blue color units display C, H, O and N atoms, respectively.

2. Experimental

2.1 Materials

N9 and N12 were synthesized in our laboratory according to our previous work.[24,25] 2,2'-Bis(trifluoromethyl)-4,4'-diaminobiphenyl (TFDB), pyromellitic dianhydride (PMDA) and N-methyl-2-pyrrolodone (NMP) were obtained from Aladdin Chemical Reagent Corp. (shanghai, China). Prior to use, PMDA was purified by recrystallization from acetic anhydride and dried under vacuum. TFDB was purified by recrystallization from toluene. NMP (semiconductor grade, 99.9%) used as received without further purification. Nematic LC E7 (n_o = 1.521, Δn = 0.22, T_{n-1} = 60 ^oC) was obtained from Yantai Xianhua Chem-Tech Co., Ltd. (Yantai, China). All the other solvents and chemicals were used as received and without further purification, unless otherwise specified.

2.2 Measurements

The spin-coat process was conducted using a KW-4A spinner from the Institute of Microelectronics of the Chinese Academy of Sciences (Beijing, China). The rubbing process was operated with a rubbing machine from TianLi Co. Ltd (Chengdu, China). Optical micrographs were obtained from polarizing optical microscope (Shanghai Millimeter Precision Instrument Co. Ltd., Shanghai, China) under room temperature with the magnification of 40 times. Surface morphology of the PI films before and after rubbing was investigated by AFM operating in tapping mode using an instrument with a SPI4000 Probe Station controller (SIINT Instruments Co., Japan) at room temperature. Olympus tapping mode cantilevers with spring constants ranging from 51.2 N m^{-1} to 87.8 N m^{-1} (as specified by the manufacturer) were used with a scan rate in the range of 0.8-1.2 Hz. Contact angles were measured by the sessile drop method using a contact angle meter (DSA100, Kruss, Hamburg, Germany), and the surface free energy was calculated by Owens's formula. The pretilt angles of LCs were measured by crystal rotation method using a pretilt angle tester from Changchun Institute of Optics, Fine Mechanics and Physics (Changchun, China), and at least five different points on cells were selected for measurement. XPS measurements were made with a Kratos XSAM800 spectrometer (Kratos Analytical Ltd., Manchester, U.K.) employing monochromatic Al K-alpha X-ray radiation (1486.6 eV). Polarized ATR-FTIR spectra were recorded on a Nicolet 560 Fourier transform spectrometer.

2.3 Synthesis of PIs

The PIs were synthesized from different functional diamines (N9 or N12) with the same ratios of PMDA and TFDB. The molar content of functional diamine was

controlled to 20%. The PIs were named as PI-N9 and PI-N12, respectively. PIs were synthesized via a conventional two-step method. The synthetic routes of all the PIs are similar, as illustrated in Fig. 2.

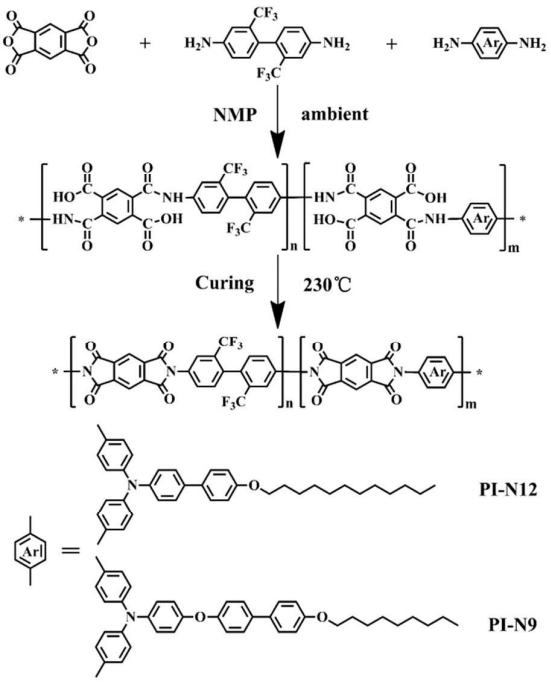

Fig. 2 Synthetic route of the polyimides.

The synthesis of PI-N9 was used as an example to illustrate the general synthetic route. The typical procedure was as follows. To a 50 mL three-necked round-bottom flask equipped with a magnetic stirrer and a nitrogen-inlet, TFDB (0.8 mmol) and N9 (0.2 mmol) were dissolved in NMP (3.35 g). After the solid was dissolved completely and a clear solution was formed, PMDA (1.0 mmol) was added, the solid content was 15%, and the mixture was stirred at room temperature under a gentle flow of dry nitrogen for 24 h. Then NMP (7.89 g) was added, the solid content was adjusted to 5%, the solution was stirred for an additional 4 h to yield moderate viscous polyamic acid (PAA) solution. Finally, PAA was thermally imidized to obtain PIs.

2.4 Preparation of PI films and assembly of LC cells

The PAA solution (5 wt% in NMP) was spin-coated on glass substrates at a rotation speed of 600 rpm for 15 s and 2500 rpm for 30 s. The films were then thermally imidized at 80 ^{o}C for 30 min, 120 ^{o}C for 30 min, 180 ^{o}C for 30 min, and 230 ^{o}C for 1 h, respectively. The prepared PI films were subsequently rubbed with a roller covered commercial rubbing cloth, and the rubbing strength (RS) was calculated as follows:

$$RS = NM\left(\frac{2\pi rn}{60v - 1}\right)$$

where RS (mm) is the total length of the rubbing cloth which contacts a certain point of the PI film; N (N=1, 2, 3……9) is the number of times the substrates were rubbed; M (0.3 mm) is the depth of the rayon velvet fabric contact with the PI film surface; v (17.2 mm/s) is the velocity of the substrate stage; n (500 rpm) is the rolling speed, and r (22.5 mm) is the radius of the roller.

The LC cells were assembled from two pieces of the rubbed glass substrates in an anti-parallel rubbing direction by using 42 μm thick PI film spacers. For comparison, some LC cells were assembled from non-rubbed glass substrates. A nematic LC (E7) was injected into the cell gap using a capillary method at 80 ^{o}C, followed by sealing of the injection hole with photo-sensitive epoxy glue. The LC cells were then heat-treated for 20 min at 80 ^{o}C, which is higher than the nematic-to-isotropic transition temperature of E7, to remove flow marks. The alignment behaviors of the LC cells were examined with polarized optical microscopy. The pretilt angles of the LC cells were measured using a crystal rotation method. Large pretilt angles near 90° were confirmed by conoscopy using a polarizing optical microscopy.

3. Results and discussion

3.1 Polarizing optical microscope observation of LC cells

In order to know whether junction mode between backbone and side chain of PI would have influence on stability of LC vertical alignment, PI-N9 and PI-N12 films were rubbed from 0 to 9 times in one direction, followed by assembling LC cells. As shown in Table 1, the pretilt angle of PI-N12 almost didn't change during the whole rubbing process; the pretilt angle of PI-N9 slight decreased when the films were rubbed less than or equal to 6 times (RS=123.41 mm), however, after being rubbed over 6 times, the pretilt angle of PI-N9 sharply decreased from 89.3° to 7.2°. The results showed that both PI-N9 and PI-N12 could induce vertical alignment when the rubbing times were less than or equal to 6. On the other hand, when the rubbing times were more than 6, PI-N9 could only induce parallel alignment but PI-N12 could still induce vertical alignment.

Table 1 Pretilt angle of the PIs films with different rubbing times

PIs	Pretilt Angle θ_p (^{o})

	0	1	2	3	4	5	6	7	8	9
PI-N12	90.0	89.9	89.9	89.9	89.9	89.9	89.9	89.9	89.9	89.8
PI-N9	90.0	89.9	89.9	89.6	89.6	89.3	89.3	7.2	7.2	7.3

The alignment behaviors of the LC cell between crossed polarizers were examined with a polarizing optical microscope (POM). As shown in Fig. 3a–f, uniform darkness was gained while the LC cell was rotated between crossed polarizers, which indicated that LCs were aligned vertical to the PI-N12 surface and the alignment was very much uniform. Meanwhile the dark crossed brush was clearly seen and didn't move with the LC cell rotating under conoscope. The results further prove that both non-rubbed and rubbed PI-N12 films can induce vertical alignment of LCs.

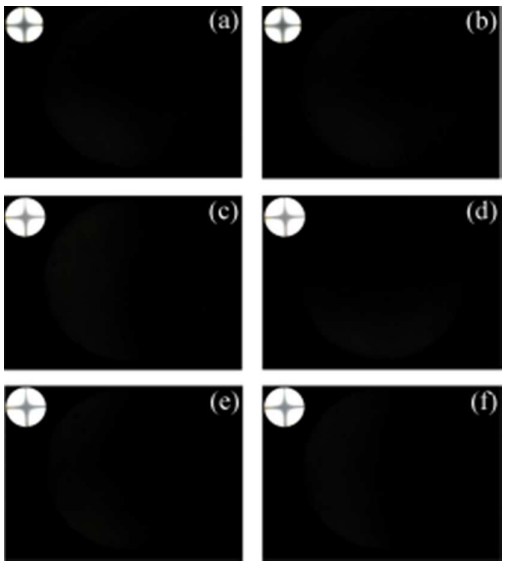

Fig. 3 The POM graphics of LC cells using the PI-N12: (a) non-rubbed, (c) six-time-rubbed, (e) seven-time-rubbed. The POM graphics of the same LC cells after rotating the stage by 45°: (b) non-rubbed, (d) six-time-rubbed, (f) seven-time-rubbed.

As shown in Fig. 4a–d, the patterns were the same as Fig. 3a-d, which revealed that PI-N9 films with the rubbing times between 0 and 6 could induce vertical alignment of LCs. However, when the rubbing times over 6, the POM graphics showed an alternate and periodic appearance of darkness and brightness, which indicated that LCs were homogeneously aligned along the rubbing direction on the surface of seven-time-rubbed PI-N9 film. The POM graphics are consistent with the results of pretilt angle. All of these confirm that the LC vertical alignment which was induced by PI-N12 film is more stable, and further prove that the vertical alignment capability

of PI-N12 film is better than that of PI-N9 film.

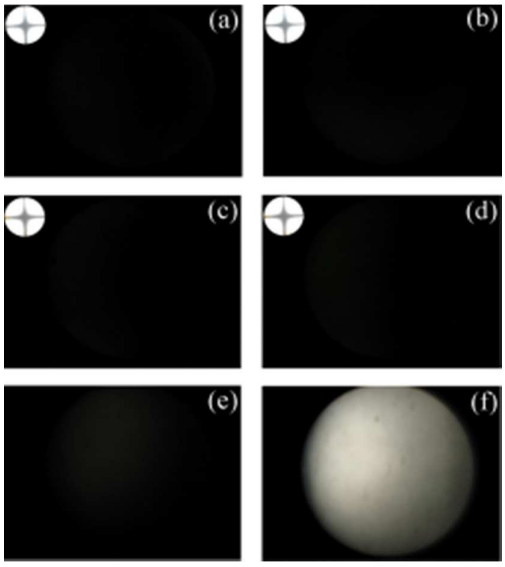

Fig. 4 The POM graphics of LC cells using the PI-N9: (a) non-rubbed, (c) six-time-rubbed, (e) seven-time-rubbed. The POM graphics of the same LC cells after rotating the stage by 45°: (b) non-rubbed, (d) six-time-rubbed, (f) seven-time-rubbed.

3.2 AFM characterization

The alignment mechanism of LC molecules on rubbed polymer films has always been the focus of researchers.[26] In order to know why the rubbing resistance of PI-N12 film is better than PI-N9 film, surface morphology of PI-N12 and PI-N9 films was measured by AFM before and after rubbing (Fig. 5). The scan size was 2.5×2.5 μm^2. Before rubbing, we can observe that the surface of PI films appeared very smooth. In addition, the root-mean-square (RMS) surface roughness of PI-N12 and PI-N9 films were 0.329 and 0.255 nm, respectively. In contrast, after rubbing, we can see that the films exhibited groove-like structures and was covered with sub-micrometer-scaled spikes along the rubbing direction, the size of microgrooves was over 35 nm, the RMS surface roughness values of the six-time-rubbed PI-N12 and PI-N9 films are 1.245 and 1.308 nm, respectively. Meanwhile the RMS surface roughness values of the seven-time-rubbed PI-N12 and PI-N9 films are 3.420 and 3.076 nm, respectively.

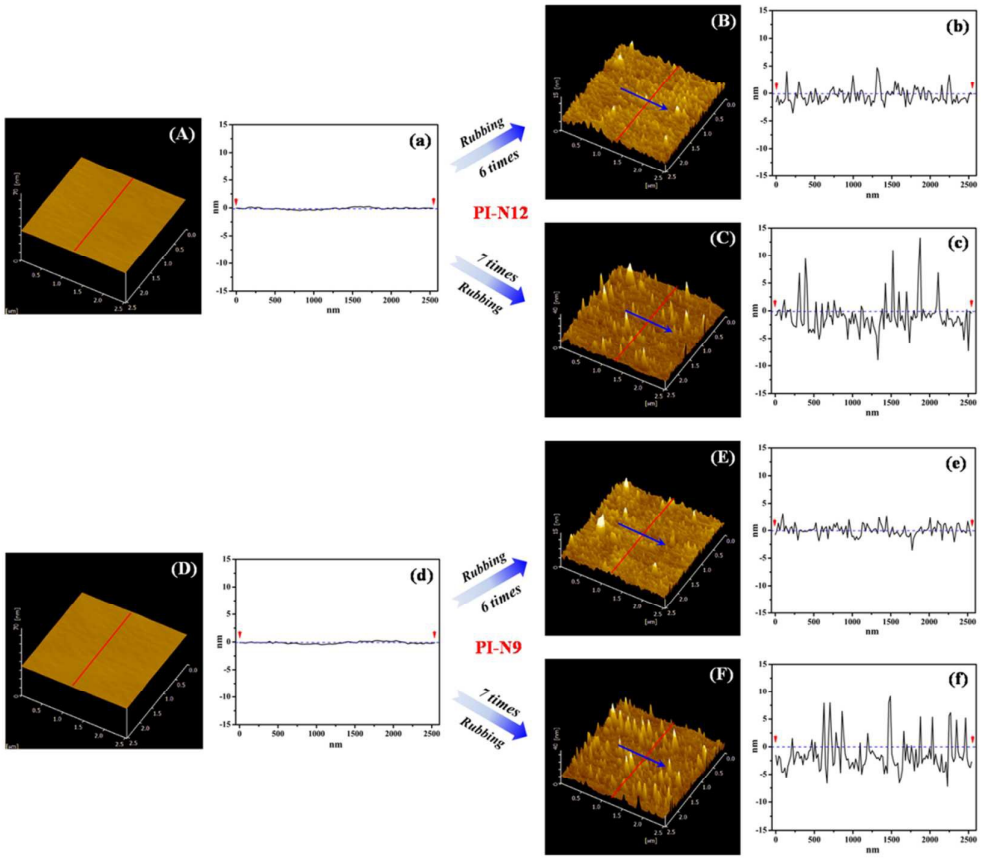

Fig. 5 The AFM graphics and surface morphology of PI films: (A) and (a) non-rubbed PI-N9 film; (B) and (b) six-time-rubbed PI-N9 film; (C) and (c) seven-time-rubbed PI-N9 film; (D) and (d) non-rubbed PI-N12 film; (E) and (e) six-time-rubbed PI-N12 film; (F) and (f) seven-time-rubbed PI-N12 film. The arrows in the graphics denote the rubbing direction.

By analyzing the surface of the alignment layer before and after rubbing, we can get results as following: First, both PI-N12 and PI-N9 films could induce vertical alignment of LCs without rubbing process. Second, although the surface morphology of PI films which had been rubbed 6 times were different from PI films without rubbing, they still could induce vertical alignment of LCs. Third, the surface morphology of PI films which had been rubbed 7 times were alike, but they induced completely different alignment behaviors of LCs (vertical alignment induced by PI-N12; parallel alignment induced by PI-N9). At last, the size of microgrooves was larger than that of LC molecules, the interaction between microgrooves and LC molecules were weak, so microgrooves couldn't ensure LC molecules are oriented entirely. Nevertheless, both side chain and LC molecule comprise aromatic unit and

aliphatic tail. Because of the similarity of chemical structure, the phenyl ring units of side chains might favorably interact with the aromatic unit of LC molecules via dipole-dipole/π-π interactions, while the alkoxy tails of side chains might undergo van der Waals type interactions with aliphatic tails of LC molecules.[4,27] From the above, it is reasonable to deduce that it is the dipole-dipole/π-π and van der Waals interactions between side chains and LC molecules that induced the alignment of LCs.

3.3 Surface free energy

The contact angles of deionized water and methylene iodide on the surface of PI films were measured. As listed in Table 2, the surface free energies were calculated by the harmonic mean equation with the rubbing times from 0 to 9, aim to analyze the relationship between the change of surface polarity of the PI films and the pretilt angle (Fig. 6).

Table 2 Surface free energy on PI surfaces with different rubbing times

Rubbing Times	Surface Energy of PI-N9 (mN/m)			Surface Energy of PI-N12 (mN/m)		
	Disperse Part	Polar Part	Total Energy	Disperse Part	Polar Part	Total Energy
0	40.15	2.81	42.96	39.38	3.49	42.86
1	39.53	3.78	43.31	40.01	3.47	43.48
2	39.73	4.52	44.26	39.96	3.88	43.83
3	39.76	4.68	44.44	39.97	4.01	43.98
4	39.90	4.33	44.23	39.32	4.85	44.17
5	39.64	4.58	44.22	39.87	4.71	44.58
6	39.69	4.97	44.66	40.35	4.53	44.88
7	41.29	5.70	46.99	39.87	4.52	44.39
8	42.10	5.25	46.16	39.64	4.75	44.40
9	41.95	5.25	47.20	39.80	4.49	44.29

In terms of the PI-N9 film, when the rubbing times were less than or equal to 6, the surface free energy and the polarity of it slightly increased with the rubbing times increasing. After rubbing over 6 times, the surface free energy obviously increased, which may resulted from the mobility of side chain. Side chains on the surface oriented out of the plane of polymer backbones before rubbing and fell over after

rubbing.[28] Therefore, the polar imide group and trifluoromethyl group were exposed on the surface of the PI-N9 films which result in an increase in the polarity of the surface of the PI-N9 film.[19]

In terms of the PI-N12 film, the surface free energy and the polarity of it slightly increased when the rubbing times increased. It is believed that alkoxy tail group oriented out of the plane of the polymer backbone and masked the polar imide group. During the rubbing process, a small amount of flexible alkoxy tail groups on the surface fell over. But the rigid benzene groups were directly linked to the polymer backbones, they didn't fall over. So the polar groups of the polymer backbone were still masked. The effect of rubbing was so weak that the PI-N12 film could still induce vertical alignment of the LCs.

However, the surface free energies of the tested PIs did not significantly change by rubbing, and this measurement can't detect precise structure of the PI film surface, so the difference of microscopic surface structure between PI-N9 and PI-N12 can't be clearly observed, thereby more accurate measurements were needed to confirm our inference.

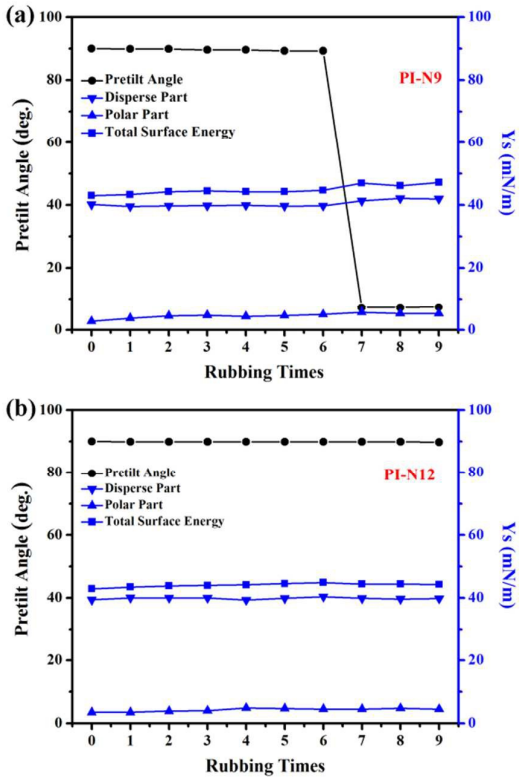

Fig. 6 The relationship between pretilt angle and surface free energy of PI-N9 (a) and

PI-N12 (b) with different rubbing times.

3.4 XPS Analysis

The chemical elements and groups in alignment film surface were characterized by XPS to investigate the change of molecular chain conformation of PI films surface. The XPS spectra of PI-N9 and PI-N12 were obtained with a take-off angle 70° (Fig. 7). The peak at 284.8 eV was assigned to the C atom linked to C atom in the alkyl chains and benzene rings (C-C or C=C). The peak at 285.8 eV was attributed to the C atom singly bonded to O atom (C-O). The peaks at 288.7eV, 292.5 eV were due to carbon-oxygen double bond (C=O), and carbon-fluorine singly bond (C-F), respectively. The relative ratio of each peak was shown in Table 3.

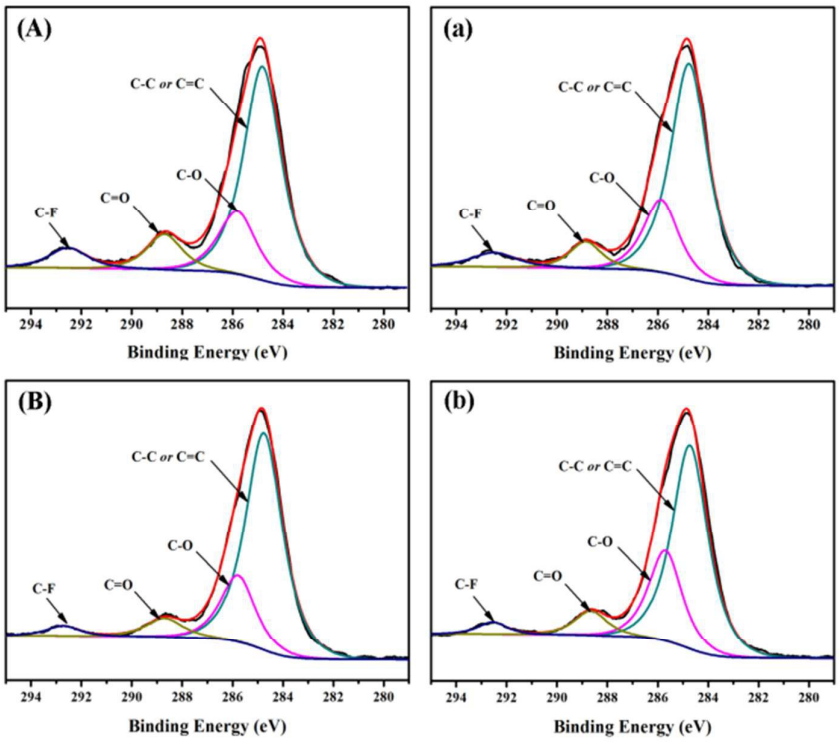

Fig. 7 The curve-fitted XPS C 1s spectra of non-rubbed PI-N9 (A), seven-time-rubbed PI-N9 (a), non-rubbed PI-N12 (B), and seven-time-rubbed PI-N12 (b).

In terms of PI-N9, the C-O only existed in the side chain, and the relative ratio of it decreased from 21.02% to 18.87% when the rubbing times varied from 0 to 7, which indicated the content of the side chain in the surface decreased. On the other hand, the C=O and C-F only existed in the backbone, and the relative ratio of them increased, which confirmed the content of backbone in the surface increased. Thus, it is reasonable to speculate that the side chains fell over and backbones were exposed on

the surface.

As a consequence, the mechanism of the macroscopic molecular orientation of the PI surface can be proposed, which was shown in Fig. 8. Comparing the chemical structure of the PI side chain, it isn't difficult to find the reason why the side chains of PI-N9 fell over easily during rubbing treatment. Due to the flexible ether bond which existed between the rigid biphenyl groups and the rigid polymer backbones, the biphenyl groups could rotate around the ether bond then fell over after rubbing, and backbones were exposed on the surface, which resulted in the content growth of C=O and C-F in the surface.

In terms of PI-N12, the rigid benzene groups in side chains were directly linked to the main chain without a flexible ether bond spacer, which restricts the movement of the whole macromolecule, thus the molecular chain conformation of PI film surface didn't change. As a result, the relative ratio of each chemical group almost had no change.

Table 3 Results of the peak separation of X-ray photoelectron spectroscope C1s spectra

PI	Atomic percentage (%)			
	C-C or C=C	C-O	C=O	C-F
Non-rubbed PI-N9	66.73	21.02	6.96	5.29
Seven-time-rubbed PI-N9	65.05	18.87	9.89	6.19
Non-rubbed PI-N12	70.73	20.22	6.07	2.98
Seven-time-rubbed PI-N12	69.72	20.28	6.95	3.05

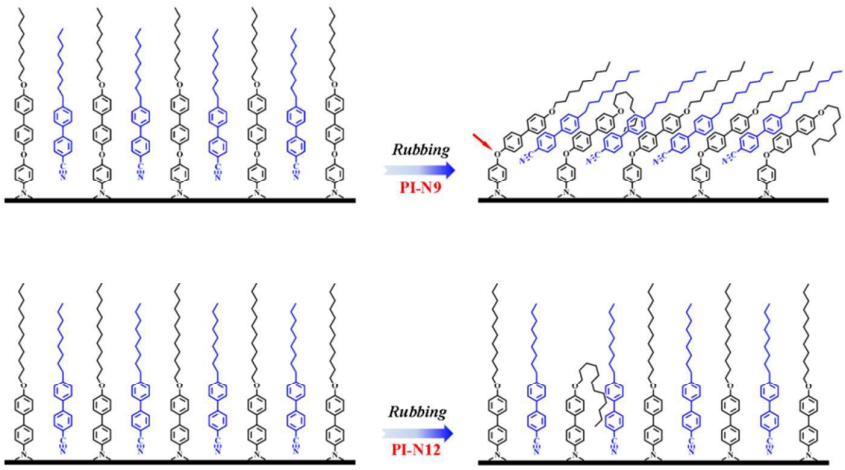

Fig. 8 Proposed mechanism of the macroscopic molecular orientation of the PI surface induced by the rubbing process.

3.5 Polarized ATR-FTIR spectra

To further understand the orientation structure in the seven-time-rubbed PIs alignment layer surface, the measurement of polarized ATR-FTIR spectra analysis was conducted. If the PI is completely random on the surface, the infrared spectra with light polarized at 0° (parallel to the plane of substrate) and 90° (normal to the plane of substrate) are identical; if the PI is oriented, these spectra are different.

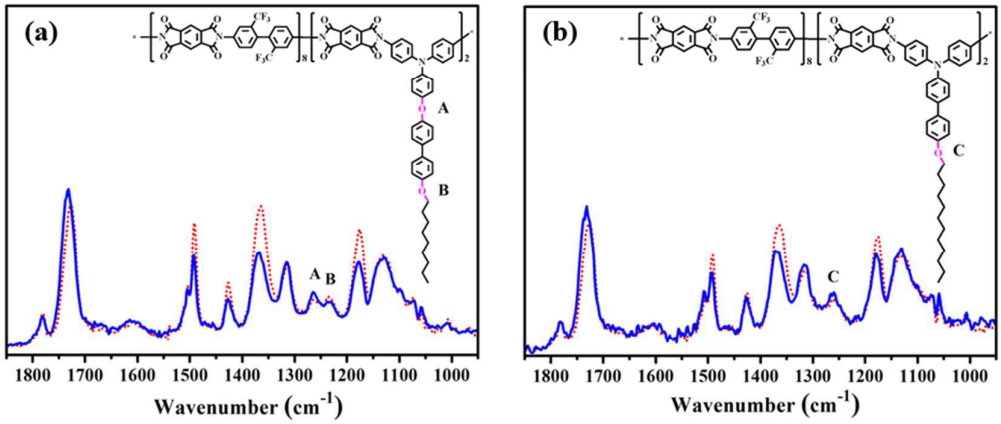

Fig. 9 Polarized ATR-FTIR spectra of seven-time-rubbed PI-N9 (a) and seven-time-rubbed PI-N12 (b). Dashed and solid lines represent the infrared spectra with light polarized at 0° (parallel to the plane of substrate) and 90° (normal to the plane of substrate), respectively.

Table 4 Spectral mode assignments for PIs

Wavenumber (cm^{-1})	Mode assignment
1728	C=O asymmetric stretching vibration of imide ring
1500	C-C stretching vibration of benzene rings skeleton
1369	C-N-C stretching vibration of imide ring
1265~1235	-O- stretching vibration of phenoxy unit
1117	C-F stretching vibration of trifluoromethyl group

The ATR-FTIR spectra of PI-N9 and PI-N12 were illustrated in Fig. 9 and mode assignments were listed in Table 4.[29-31] As is mentioned above, PI-N9 and PI-N12 have the same backbone which is composed of benzene unit, imide ring and trifluoromethyl. When the direction of polarization was changed from 0° to 90°, the

absorptions at 1369 and 1117 cm^{-1} decreased sharply, which revealed that imide ring and trifluoromethyl favorably oriented parallel to the plane of substrate. In addition, due to the molar content of side chains was only 20%, the increase of absorption at about 1500 cm^{-1} could be mainly attributed to benzene rings in backbone. All these groups lie along the backbone axis, which mean that the backbone favorably oriented parallel to the plane of substrate. On the contrary, the absorption of C=O of imide ring slightly increased which suggested that C=O might deviate from backbone axis. This is consistent with the former researcher's results.[4] According to the literature reported, an inter-ring torsion angle might between the imide ring and the benzene ring, and the C=O is perpendicular to the backbone axis and orient out of plane of the film.[4,19,23] Taken together, we can preliminarily conclude that the backbone tended to adopt parallel reorientation.

Although the shapes of most peaks were similar, the peaks at 1265~1235 cm^{-1} exhibited obvious difference. In the spectra of seven-time-rubbed PI-N9 (Fig. 9a), there were two peaks appearing. They were peak A and B at 1265 and 1235 cm^{-1}, respectively. Nevertheless, for PI-N12, only a peak C appeared at 1260 cm^{-1} (Fig. 9b). This may result from the different side chains structure of PI-N9 and PI-N12. Commonly, the absorption of C-O appears at 1250~1050 cm^{-1}. In our case, because of the p-π conjugation, the absorption of C-O shifted to higher wave number. Therefore, the peaks at 1265~1235 cm^{-1} were assigned to C-O. For PI-N9, there were two kinds of C-O in its side chain, one connected with benzene and biphenyl (peak A), and another connected with biphenyl and alkyl chain (peak B); for PI-N12, the side chain contained only one kind of C-O which connected with biphenyl and alkyl chain (peak C). When the direction of polarization was changed from 0° to 90°, the intensity of peak A increased while the intensity of peak B decreased, which indicated that the ether bond connected with benzene and biphenyl was preferentially reoriented normal to the plane of substrate and the ether bond connected with biphenyl and alkyl chain was preferentially reoriented parallel to the plane of substrate. The results confirmed that biphenyl groups rotated around the ether bond then fell over and adopted parallel reorientation after high-strength rubbing. On the other hand, the intensity of peak C increased clearly under the same condition. This demonstrated that the C-O of PI-N12 tended to adopt vertical reorientation.

These spectral differences proved that the side chains of PI-N9 were preferentially reoriented parallel to the plane of substrate while the side chains of PI-N12 were

preferentially reoriented normal to the plane of substrate. Meanwhile, according to the former literature,[4,23,27] because of the similarity of side chain structure and LC molecule, there are some intermolecular interactions existing between LC molecules and side chains of PIs, such as the dipole-dipole and π-π interaction between the biphenyl groups of LC molecules and the biphenyl groups of side chains, and the van der Waals forces between the alkoxy end-group of PI and the flexible alkoxy tail in LC molecule. Due to these strong interactions, LC molecules tend to be aligned in the direction parallel to the side chains of polyimide, thereby generating alignment of LCs. The results also further confirm the mechanism of the macroscopic molecular orientation of the PIs surface which was illustrated in Fig. 8 is reasonable.

4. Conclusions

Two kinds of PIs were synthesized from different functional diamines (N9 or N12) with the same ratios of TFDB, and PMDA to investigate the effect of junction mode between backbone and side chain of PI on stability of LC alignment. According to measurements above, we can infer that the vertical alignment of LC was mainly effected by the reorientation of side chains of PIs rather than the microgrooves which were produced by rubbing. Since the side chain was linked to the backbone in different ways (for PI-N9, linked with an ether bond spacer; for PI-N12, directly linked without any spacer), the side chain of PI-N12 could tolerant high-strength rubbing，while PI-N9 could not. The results mean that junction mode between backbone and side chain plays an important role in achieving stable vertical alignment of liquid crystals. Besides, the mechanism of the macroscopic molecular orientation of the PIs surface is proposed. Due to the flexible ether bond which existed between the side chain and the main chain of PI-N9, during high-strength rubbing process, the side chain could rotate around the ether bond then fell over. The PI-N9 could not induce the vertical alignment of LCs anymore. On the other hand, the mobility of side chains of PI-N12 was restricted by rigid PI main chains. So PI-N12 could keep LCs aligning vertically all the time, which proved that the stability of LC alignment induced by PI-N12 was better than that induced by PI-N9.

Acknowledgements

This work was supported by National Natural Science Foundation of China (Grant no.

51173115), the Ministry of Education (the Foundation for Ph.D. training, Grant no. 20110181110030) of China. We acknowledge Prof. Mingbo Yang and Chengdu Institute of Organic Chemistry, Chinese Academy of Sciences for characterization.

References

[1] D. Liawa, K. Wang, Y. Huang, K. Lee, J. Lai and C. Ha, *Progress in Polymer Science*, 2012, **37**, 907.

[2] B. Zhang, Y. Chen, Y. Zhang, X. Chen, Z. Chi, J. Yang, J. Ou, M. Q. Zhang, D. Li, D. Wang, M. Liu and J. Zhou, *Phys. Chem. Chem. Phys.*, 2012, **14**, 4640.

[3] H. L. Lee, O. H. Kwon, S. M. Ha, B. G. Kim, Y. S. Kim, J. C. Won, J. Kim, J. H. Choic and Y. Yoo, *Phys. Chem. Chem. Phys.*, 2014, **16**, 20041.

[4] S. Lee, S. Lee, S. Hahm, T. Lee, B. Lee, B. Chae, S. Kim, J. Jung, W. Zin, B. Sohn and M. Ree, *Macromolecules*, 2005, **38**, 4331.

[5] B. Lee, G. Shin, J. Chi, W. Zin, J. Jung, S. Hahm, M. Ree and T. Chang, *Polymer*, 2006, **47**, 6606.

[6] S. Noh, K. Araki and M. Seno, *J. Mater. Chem.*, 1993, 7, 755

[7] J. Hoogboom, T. Rasing, A. Rowan and R. Nolte, *J. Mater. Chem.*, 2006, **16**, 1305.

[8] H. Long and D. Yoon, *Mat. Res. Soc. Symp. Proc.*, 1994, **345**, 247.

[9] K. Sakamoto, R. Arafune, N. ITo, S. Ushioda, Y. Suzuki and S. Morokawa, *Jpn. J. Appl. Phys.*, 1994, **33**, 1323.

[10] B. Chae, S. Kim, S. Lee, S. Kim, W. Choi, B. Lee, M. Ree, K. Lee and J. Jung, *Macromolecules*, 2002, **35**, 10119.

[11] J. Naciri, D. Shenoy, K. Grueneberg and R. Shashidha, *J. Mater. Chem.*, 2004, **14**, 3468.

[12] K. Lee, A. Lien, J. Stathis and S. Paek, *Jpn. J. Appl. Phys.*, 1997, **36**, 3591.

[13] C. Cai, A. Lien, P. Andry, P. Chaudhari, R. John, E. Galligan, J. Lacey, H. Ifill, W. Graham and R. Allen, *Jpn. J. Appl. Phys.*, 2001, **40**, 6913.

[14] H. Vithana, D. Johnson, P. Bos, R. Herke, Y. Fung and S. Jaml, *Jpn. J. Appl. Phys.*, 1996, **35**, 2222.

[15] Z. Liu, F. Yu, Q. Zhang, Y. Zeng and Y. Wang, *Eur. Polym. J.*, 2008, **44**, 2718.

[16] B. Chae, S. Lee, B. Lee, W. Choi, S. Kim, Y. Jung, J. Jung, K. Lee and M. Ree, *Langmuir*, 2003, **19**, 9459.

[17] Y. G. Kang, H. J. Kim, H. G. Park, B. Y. Kim and D. S. Seo, *J. Mater. Chem.*,

2012, **22**, 15969.

[18] Y. T. Chern and M. H. Ju, *Macromolecules*, 2009, **42**, 169.

[19] T. Sakai, K. Ishikawa and Hideo Takezoe, *Liq. Cryst.*, 2002, **29**, 47.

[20] Y. Lee, J. Choi, I. Song, J. Oh and M. Yi, *Polymer*, 2006, **47**, 1555.

[21] C. Guo, Z. Sun, S. Xia and Y. Wang, *Liq. Cryst.*, 2012, **39**, 721.

[22] X. Wang, P. Zhang, Y. Chen, L. Luo, Y. Pang and X. Liu, *Macromolecules*, 2011, **44**, 9731.

[23] K. Takizawa, J. Wakita, M. Kakiage, H. Masunaga and S. Ando, *Macromolecules*, 2010, **43**, 2115.

[24] S. Gong, M. Liu, Z. Sun, S. Xia and Y. Wang, *Liq. Cryst.*, 2014, **41**, 1831-1842.

[25] M. Liu, X. Zheng, S. Gong, L. Liu, Z. Sun, L. Shao and Y. Wang, *RSC Adv.*, 2015, **5**, 25348.

[26] H. M. Wu, J. H. Tang, Q. Luo, Z. M. Sun, Y. M. Zhu, Z. H. Lu and Y. Wei, *Appl. Phys. B.*, 1996, **62**, 613.

[27] H. Kang, J. S. Park, E. Sohn, D. Kang, C. Rosenblatt and J. Lee, *Polymer*, 2009, **50**, 5220.

[28] K. Lee, S. Paek, A. Lien, C. Durning and H. Fukuro, *Macromolecules*, 1996, **29**, 8894.

[29] H. Ishida, S. T. Wellinghoff, E. Baer and J. L. Koenig, *Macromolecules*, 1980, **13**, 826.

[30] K. Sakamoto, R. Arafune, N. Ito, S. Ushioda, Y. Suzuki and S.J. Morokawa, *Appl. Phys.*, 1996, **80**, 431.

[31] R. Nuzzo, L. Dubois, and D. Allara, *J. Am. Chem. Soc.*, 1990, **112**, 558.